Feasibility of two low-cost organic substrates for inducing denitrification in artificial recharge ponds: Batch and flow-through experiments

Alba Grau-Martínez [(a,*)], Clara Torrentó [(a,b)], Raúl Carrey [(a)], Paula Rodríguez-Escales [(C)], Cristina Domènech [(a)], Giorgio Ghiglieri [(d,e)], Albert Soler [(a)], Neus Otero [(a)]

(a) Grup de Mineralogia Aplicada i Geoquímica de Fluids, Departament de Mineralogia, Petrologia i Geologia Aplicada, SIMGEO UB-CSIC, Facultat de Geologia, Universitat de Barcelona (UB), C/ Martí i Franquès, s/n - 08028 Barcelona, Spain. albagrau@ub.edu, clara.torrento@ub.edu, raulcarrey@ub.edu, cristina.domenech@ub.edu, albertsoler@ub.edu, notero@ub.edu
(b) Centre for Hydrogeology and Geothermics, University of Neuchâtel, 2 Rue Emile-Argand 11, 2000 Neuchâtel, Switzerland. clara.torrento@unine.ch
(c) Hydrogeology Group (GHS). Departament of Civil and Environmental Engineering, Universitat Politècnica de Catalunya (UPC), c/Jordi Girona 1-3, 08034 Barcelona, Spain. paula.rodriguez.escales@upc.edu
(d) Department of Chemical and Geological Sciences, University of Cagliari, Via Trentino 51, 09127 Cagliari, Italy. ghiglieri@unica.it
(e) Desertification Research Center-NRD, University of Sassari, Viale Italia 39 – 07100 Sassari, Italy

 (*) Corresponding author: Alba Grau-Martínez
e-mail: albagrau@ub.edu
Fax: +34 93 402 13 40.
Phone: +34 93 403 37 73 ext: 33773

FEASIBILITY OF TWO LOW-COST ORGANIC SUBSTRATES FOR INDUCING DENITRIFICATION IN ARTIFICIAL RECHARGE PONDS: BATCH AND FLOW-THROUGH EXPERIMENTS

Alba Grau-Martínez[a*], Clara Torrentó[a,b], Raúl Carrey[a], Paula Rodríguez-Escales[c], Cristina Domènech[a], Giorgio Ghiglieri[d,e], Albert Soler[a], Neus Otero[a]
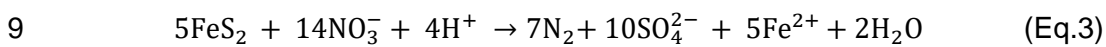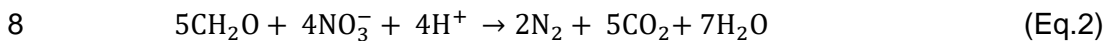
Keywords

1. Introduction

Nitrate (NO_3^-) contamination of groundwater usually originates from anthropogenic sources (mainly intensive application of fertilisers and animal manure), and is a major environmental problem that affects several regions of the world (Spalding and Exner, 1993). It is not unusual for groundwater NO_3^- concentrations to exceed the nominal limit of 50 mg L^{-1} for drinking water set by the 98/83/EC European Union Council Directive. High NO_3^- ingestion can cause methemoglobinaemia in infants and young children (Magee and Barnes, 1956) and may also promote stomach cancer. Although NO_3^- contamination of aquifers is a serious environmental and health issue, natural denitrification can occur, reducing pollution levels and diminishing the severity of the problem. This process is considered to be the most important reaction that attenuates NO_3^- in groundwater (Knowles, 1982). Denitrification may be defined as the dissimilatory microbial reduction of NO_3^- to nitrogen gas (N_2) through several intermediate steps (Eq. 1).

$$NO_3^- \rightarrow NO_2^- \rightarrow NO \rightarrow N_2O \rightarrow N_2 \qquad (Eq.1)$$
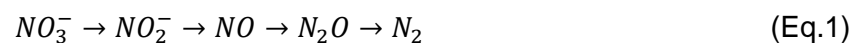
Denitrification takes place under anaerobic conditions where bacteria use NO_3^- as an oxidant for different materials such as organic matter, sulphides and iron minerals.

1 Denitrification can proceed by the action of heterotrophic or autotrophic bacteria, which

2 oxidise organic or inorganic substrates, respectively (simplified Eq. 2, 3). In both cases,

3 NO_3^- is first transformed into nitrite (NO_2^-), which is actually more toxic than NO_3^- (DeBeer

4 et al., 1997), with a maximum concentration in drinking water of 0.46 mg L^{-1} (Directive

5 98/83/CE). Through successive steps, NO_2^- is transformed into nitric oxide (NO), which

6 can further be reduced to nitrous oxide (N_2O); both species are considered greenhouse

7 gases. Finally, N_2O is converted to harmless N_2.

8 $$5CH_2O + 4NO_3^- + 4H^+ \rightarrow 2N_2 + 5CO_2 + 7H_2O \qquad (Eq.2)$$

9 $$5FeS_2 + 14NO_3^- + 4H^+ \rightarrow 7N_2 + 10SO_4^{2-} + 5Fe^{2+} + 2H_2O \qquad (Eq.3)$$

10 Under anaerobic conditions, nitrate may also be reduced to ammonium (NH_4^+) by a

11 process known as dissimilatory NO_3^- reduction to NH_4^+ (DNRA or ammonification). DNRA

12 is induced by fermentative bacteria, reducing NO_3^- to NO_2^- before a final reduction to

13 NH_4^+ (Tiedje et al., 1982).

14 When anoxic or hypoxic conditions are guaranteed, the main limitation of natural

15 attenuation of NO3- is the lack or limited availability of electron donors (Knowles, 1982).

16 Furthermore, the presence of inorganic electron donors, such pyrite, is not abundant.

17 Thus, both autotrophic and heterotrophic denitrification processes are usually limited.

18 For this reason, the most common strategy to remediate NO_3^- contamination from point

19 source discharges has been the addition of an external electron donor into the system in

20 order to enhance the capacity of indigenous denitrifying biomass to reduce NO_3^- into

21 dinitrogen gas (Leverenz, et al., 2010; Vidal-Gavilan, et al., 2013). For economical,

22 practical and environmental reasons, an organic carbon source is the most common

23 external electron donor added to the system. Organic carbon can be incorporated into

24 the aquifer via active systems such as injection wells (e.g. Vidal-Gavilan et al., 2013) or

25 passive systems such as permeable reactive barriers, PRBs (Gibert et al., 2008;

26 Robertson et al., 2008).

27 In arid and semi-arid regions, managed aquifer recharge (MAR) is a widely used

28 technique to increase water supplies. Infiltration and artificial recharge are achieved by

1 ponding or flowing water on the soil surface with basins, furrows, ditches or ponds

2 (Bouwer, 2002). Artificial recharge ponds (ARP) require excavation of permeable terrain

3 close to the water source (river channel, effluent from a water treatment plant (WTP),

4 etc.). A decantation pond is often included in these systems to improve water quality

5 through deposition of suspended solids. Additionally, in order to improve the quality of

6 both recharged and groundwater, the infiltration ponds can be coupled with a PRB, e.g.

7 an organic reactive layer at the bottom of the pond. The release of organic carbon into

8 the system is expected to enhance endogenous microbiology activity, improving the

9 natural attenuation rate of some target pollutants.

10 A good example of ARP coupled with PRB is located in Sant Vicenç dels Horts

11 (Barcelona, Spain), where the aquifer is recharged by Llobregat River water. Several

12 studies have shown that the organic reactive layer in this ARP has improved elimination

13 of some organic contaminants (Valhondo et al., 2014). One of the key design parameters

14 in ARP-PRB facilities is the type of material in the reactive layer. This should be effective,

15 economic and easily available. Furthermore, it must be adapted to the socioeconomic

16 circumstances of each country. In several source water used for MAR purposes, such

17 as treated wastewater, the presence of not only NO_3^-, but also NH_4^+, N-organic

18 compounds and other organic micropollutants, might affect the suitability of these

19 sources for using as recharge water (Miller et al., 2006; Díaz-Cruz and Barceló, 2008;

20 Kuster et al., 2010; Maeng et al., 2011). The main organic N-containing compounds

21 present in effluents of water treatment plants are amino acids,

22 ethylenediaminetetraacetic acid (EDTA), disinfection by-products, humic substances,

23 pharmaceuticals and pesticides (Pehlivanoglu-Mantas and Sedlak, 2008; Westgate and

24 Park, 2010). Therefore, MAR might significantly lower the concentration of these

25 contaminants present in the source water (Bekele et al., 2011). For sustainable

26 groundwater management, the attenuation and fate of these compounds in groundwater

27 environments during MAR must be evaluated for each specific recharge site.

28 In the framework of the project entitled "Water harvesting and Agricultural techniques in

1   Dry lands: an Integrated and Sustainable model in Maghreb Regions" (WADIS-MAR,

2   www.wadismar.eu) a MAR system consisting of ARP with an organic reactive layer will

3   be installed in the Maghreb region (in the watersheds of Oued Biskra, Algeria). The area

4   is characterized by poor soil development, low organic matter content, water scarcity,

5   increasing water demand, overexploitation of groundwater resources and high exposure

6   to nitrate contamination. In this area, recharge is mainly due to short, heavy floods

7   caused by erratic and intense short-term rainfall events (Ghiglieri et al., 2014). Before

8   implementing the ARP in the Maghreb region, laboratory feasibility tests were carried out

9   to select the best viable substrate for the reactive layer and to evaluate its capacity to

10   remove NO_3^- . Several organic substrates, such as compost and softwood, had

11   previously been evaluated for their use in denitrification PRBs (Gibert et al., 2008). In

12   this study, we sought to identify low-cost, easily available and easily handled organic

13   substrates with the capacity to rapidly enhance denitrification in reactive layers in ARPs

14   located in arid and semi-arid regions, where groundwater recharge periods are typically

15   short. Bearing the above criteria in mind, we selected palm tree leaves and compost, the

16   former because palm trees are typical flora in arid North African regions and the latter to

17   serve for comparison with ARPs in moderate to humid regions such as Sant Vicenç dels

18   Horts.

19   Isotopic studies coupled with chemical data are an effective tool to identify and describe

20   denitrification (Aravena and Robertson, 1998). Furthermore, multi-isotopic studies of the

21   solutes involved in the reactions, such as the $\delta^{13}C$ of dissolved inorganic carbon and the

22   $\delta^{34}S$ and $\delta^{18}O$ of dissolved sulphate, can help determine whether denitrification is

23   promoted by heterotrophic or autotrophic bacteria and identify the existence of

24   secondary processes such as SO_4^{2-} reduction (Mariotti et al., 1988).

25   The major goal of this study was therefore to assess the denitrification capacity of two

26   substrates for their potential use in ARPs. To this end, laboratory batch and column

27   experiments were performed. The possible adverse effects, such as NO_2^- accumulation,

28   NH_4^+ formation and sulphate reduction, were also considered and characterised using

isotopic and modelling tools. The second goal of this study was to obtain the nitrogen

and oxygen isotope fractionations associated with the studied degradation processes to

evaluate their potential use as a tool for assessing the efficiency of future enhanced

denitrification activities at field scale.

2. Experimental set-up and methods

2.1. Experimental set-up

Batch and flow-through experiments were performed with the two materials tested,

commercial compost from a composting plant located in Moià (Catalonia, NE Spain) and

palm tree leaves from the Maghreb region (the watersheds of Oued Biskra in Algeria).

Both substrates consisted of irregular pieces of organic material between 0.3 and 2 cm

in size and were used without any specific pre-treatment. The amount of N and C (%) as

well as the $\delta^{15}N$ (‰) and $\delta^{13}C$ (‰) of both substrates was characterised (Table 1).

The groundwater used in all the experiments was from the Llobregat aquifer. This was

chosen because it is chemically comparable (Soler et al. 2016) to the watersheds of

Oued Biskra in Algeria groundwater and it significantly facilitated and reduced the cost

of the experiment. All the experiments were performed in a glove box with an argon

(batch experiments) or nitrogen (flow-though) atmosphere to avoid the presence of O_2.

Experimental oxygen partial pressure in the glove box was maintained between 0.1%

and 0.3% O_2, and was continuously monitored by an oxygen partial pressure detector

(Sensotran, Gasvisor 6) with an accuracy of ±0.1% O_2.

Four types of batch experiment were performed in sterilised 500 mL glass bottles.

Groundwater, spiked with $NaNO_3$ in varying amounts, was added to the glass bottles

(Table 2). Commercial compost batch (CCB) and palm tree leaves batch (PTB)

experiments were run in triplicate using the selected material and groundwater spiked

with 0.80 mM of NO_3^- previously purged with N_2 for 15 min. A 'sterilised control'

experiment (SCB) was carried out adding autoclaved material (palm tree leaves) to

autoclaved groundwater which had been previously degassed. In addition, an 'absence

control' experiment (ACB) was carried out using only degassed groundwater. Batch experiments with palm tree leaves lasted for 24 hours, whereas those with commercial compost lasted 11 days. In the case of the experiments with compost, bottles were manually shaken once a day while in the case of the experiments with palm tree leaves, bottles were shaken before each sampling event. Aqueous samples (5 mL) were periodically collected using sterile syringes. The number of samples was limited to maintain the solution: solid material ratio at 90% of initial value.

The two flow-through experiments were carried out using glass cylindrical columns (35 cm high, 9 cm inner diameter) (Supplementary material, Figure S1). The commercial compost column (CCC) was filled with 1.24 kg of compost mixed with 3.34 kg of clean silica sand (Panreac®) to increase permeability and prevent flotation of the reactive material. The palm tree column (PTC) was filled with 134 g of palm tree leaves mixed with 3.36 kg of clean silica sand. Thus, total organic C was 40.6 and 18.2 g kg^{-1} for CCC and PTC experiments, respectively. In both experiments, the bottom of the column was filled with silica balls (2 mm Ø) to prevent sediment clogging the outlet. From the results of a bromide tracer test performed just before the start of the experiments, porosity (45% and 28%) and pore volume (0.77 L and 0.52 L) were estimated for the CCC and the PTC experiments, respectively. The columns were filled with water leaving a 4.5 cm free nappe over the sediment to prevent the occurrence of a preferential flow pathway. Both columns operated in downflow mode and the flow rate was controlled by a peristaltic pump (Micropump Reglo Digital 4 channels ISMATEC). In both experiments, two stages were defined separated by a lag period with no flow during which the columns were dried and kept in the glove box. This lag period was used to simulate a dry period in an artificial recharge set-up. During both stages (I and II), flow rate varied from 0.2 mL min^{-1} to 0.4 mL min^{-1}. The duration and flow rates of each stage are detailed later in this paper for the CCC and PTC experiments, respectively. The input water was spiked with a NaNO$_3$ solution to achieve a known nitrate concentration of between 0.8 mM and 2.9 mM for the CCC experiment and between 0.7 mM and 3.5 mM for the PTC experiment.

1 Both flow-through experiments lasted over 7 months and 76 and 56 samples were

2 collected from the outlet of the CCC and PTC, respectively.

3 **2.2. Analytical methods**

4 Anion (NO_3^-, NO_2^-, Cl^- and SO_4^{2-}) concentrations and isotope ratios ($\delta^{15}N$ and $\delta^{18}O$ of

5 dissolved NO_3^-) were measured in all the batch experiment samples. In the flow-through

6 experiments, anions, cations, NH_4^+, non-purgeable dissolved organic carbon (NPDOC)

7 and dissolved inorganic carbon (DIC) were measured, and isotopic data were

8 determined for a subset of samples considered representative according to the

9 measured concentration of the target analyses. Redox potential (Eh) and pH were

10 measured daily at the column outflow with portable electrodes (WTW-3310). Aliquots of

11 aqueous samples were filtered through 0.2 µm Millipore® filters. Anion concentration was

12 determined by high performance liquid chromatography (HPLC) with a WATERS 515

13 HPLC pump, IC-PAC anion columns and a WATERS 432 detector. For major cation

14 analysis, samples were acidified with 1% HNO_3^-. Cation concentrations were determined

15 by inductively coupled plasma-optical emission spectrometry (ICP-OES, Perkin-Elmer

16 Optima 3200 RL). NH_4^+ was analysed using ionic chromatography (DIONEX, ICS5000).

17 NPDOC was measured by organic matter combustion using a MULTI N/C 3100 Analytik

18 Jena carbon analyser. Periodically, 25 mL of aqueous solution was sampled to measure

19 dissolved inorganic carbon (DIC) by titration (METROHM 702 SM Titrino). Chemical

20 analyses were conducted at the the "Centres Científics i Tecnològics" of the Universitat

21 de Barcelona (CCiT-UB).

22 Stable isotopes are usually measured as the ratio between the heavier isotope (e.g.^{15}N)

23 and the lighter isotope (e.g.^{14}N). These ratios are referenced to international standards

24 using delta notation (δ), which is used to express the small variations in isotopic

25 composition that occur and is defined by Eq. 4, where $R = {}^{15}N/{}^{14}N$.

26
$$\delta^{15}N = \left[(R_{sample} - R_{std}) \big/ R_{std} \right] \times 1000 \qquad \text{(Eq.4)}$$

1 The isotopic analyses included the $\delta^{15}N$ and $\delta^{18}O$ of NO_3^-, $\delta^{15}N$ of NH_4^+, $\delta^{34}S$ and $\delta^{18}O$

2 of SO_4^{2-}. The $\delta^{15}N$ and $\delta^{18}O$ of dissolved NO_3^- were determined using a modified

3 cadmium reduction method (McIlvin and Altabet, 2005; Ryabenko et al., 2009). Briefly,

4 NO_3^- was converted to NO_2^- through spongy cadmium reduction and then to nitrous oxide

5 using sodium azide in an acetic acid buffer. Simultaneous $\delta^{15}N$ and $\delta^{18}O$ analysis of the

6 N_2O produced was carried out using a Pre-Con (Thermo Scientific) coupled to a Finnigan

7 MAT-253 Isotope Ratio Mass Spectrometer (IRMS, Thermo Scientific). The $\delta^{15}N$ of NH_4^+

8 was analysed by the NH_4^+ diffusion method using a Carlo Erba Elemental Analyser (EA)

9 coupled in a continuous flow to a Finnigan Delta C IRMS (Thermo Scientific). For $\delta^{34}S$

10 and $\delta^{18}O$ analyses, dissolved SO_4^{2-} was precipitated as $BaSO_4$ by adding $BaCl_2 \cdot 2H_2O$

11 after acidifying the sample with HCl and boiling it to prevent $BaCO_3$ precipitation,

12 following standard methods (Dogramaci et al., 2001). The $\delta^{34}S$ was also analysed with

13 the Carlo Erba EA -Finnigan Delta C IRMS. The $\delta^{18}O$ was analysed in duplicate using a

14 ThermoQuest high temperature conversion elemental analyser (TC/EA) coupled in

15 continuous flow with a Finnigan MAT Delta C IRMS. For $\delta^{13}C_{DIC}$, carbonates were

16 converted to CO_2 gas by adding a phosphoric acid solution and the isotope ratio was

17 measured in a Gas-Bench II coupled to a MAT-253 IRMS (Thermo Scientific). The $\delta^{13}C$

18 and $\delta^{15}N$, as well as total C (%), of the two tested organic substrates were measured

19 using the Carbo Erba EA-Finnigan Delta C IRMS. Isotope ratios were calculated using

20 both international and internal laboratory standards. Notation was expressed in terms of

21 δ relative to the international standards (V-SMOW for $\delta^{18}O$, atmospheric N_2 for $\delta^{15}N$ and

22 V-CDT for $\delta^{34}S$). The reproducibility of the samples was ±1‰ for the $\delta^{15}N$ of NO_3^-, ±0.5‰

23 for the $\delta^{15}N$ of NH_4^+, ±1.5‰ for the $\delta^{18}O$ of NO_3^-, ±0.2‰ for the $\delta^{34}S$ of SO_4^{2-} and ±0.5‰

24 for the $\delta^{18}O$ of SO_4^2. Samples for isotopic analyses were prepared at the "Mineralogia

25 Aplicada I Geoquímica de Fluids" laboratory and determined at the "Centres Científics i

26 Tecnològics" of the Universitat de Barcelona (CCiT-UB).

27

28

2.3. Isotope data evaluation

Isotopic fractionation during denitrification can be expressed as a Rayleigh distillation process (Eq. 5), from which the isotopic fractionation factor α can be obtained (Mariotti et al., 1988; Aravena and Robertson, 1998).

$$Ln\left(R_t/R_0\right) = (\alpha - 1) * Ln\left(C_t/C_0\right)$$ (Eq.5)

where C_0 and C_t are the initial and residual NO_3^- concentrations, respectively (mmol L^{-1}), and R_0 and R_t denote the ratios of heavy versus light isotopes in the initial and residual isotopic ratios, respectively, which are calculated according to Eq. 6.

$$R = \left[\left(\delta/1000\right) + 1\right]$$ (Eq.6)

where δ is the isotopic composition of $\delta^{15}N$ and $\delta^{18}O$ (‰). The term (α - 1) was calculated from the slope of the regression analysis in double-logarithmic plots [ln(R_t/R_0)] over [ln(C_t/C_0)] according to Eq. 5, and converted to isotopic fractionation (ε_N and ε_O) according to Eq. 7.

$$\varepsilon = 1000 \times (\alpha - 1)$$ (Eq.7)

The Rayleigh equation applies to closed system conditions; therefore, isotopic fractionation is commonly calculated in laboratory experiments where conditions are well constrained, no other sinks affect the NO_3^- pool and the concentration and isotopic composition of NO_3^- can be considered exclusively determined by NO_3^- reduction.

3. Results

Results of the batch experiments are detailed in supplementary material Table S1, and results of the flow through experiments are detailed in Tables S2-S5.

3.1. Batch experiments: chemical data

In the sterilised control (SCB) and absence control (ACB) experiments, NO_3^- reduction did not occur. Results for CCB experiments showed complete NO_3^- consumption in less than 12 days (Fig. 1a). At t=0 (right after the groundwater spiked with NaNO3 was put in contact with the commercial compost) an initial NO3- release by the compost of up to

1 2.58 mM was observed. In the palm tree batch experiment (PTB), complete NO_3^-

2 reduction was achieved in less than 20 hours with no significant initial NO_3^- release (Fig.

3 1b). In both batch experiments, transient NO_2^- accumulation was observed. In the CCB

4 experiment, up to 0.1 mM of NO_2^- was released on the first day, and thereafter NO_2^-

5 concentration gradually decreased. In the PTB experiment, NO_2^- transient accumulation

6 was more significant, with a concentration peak of 0.7 mM after 14 hours, which

7 corresponds to 81% of the initial NO_3^- concentration. NO_2^- content was negligible after 22

8 hours.

9

10 **3.2. Flow-through experiments: chemical data**

11 Results for the evolution of NO_3^-, NO_2^-, NH_4^+, SO_4^{2-}, NPDOC and DIC during the flow-

12 through experiments are shown in Figures 2 (CCC) and 3 (PTC). The CCC experiment

13 was characterised by a large initial NO_3^- release (up to 4.3 mM) in the first 4 days of

14 stage I. This NO_3^- was released due to leaching from the compost, similarly to what was

15 observed in the CCB experiment. After that, complete NO_3^- consumption was achieved.

16 The decrease in NO_3^- concentration was coupled with a slight increase in NO_2^-, which

17 reached values of up to 1.3 mM in the first 7 days. A slight NH_4^+ concentration was

18 detected in the output (values between 0.03 μM and 0.4 mM, Fig. 4a). The SO_4^{2-}

19 concentration in the input water was 1.9 mM, and in the outflow water it ranged from 0.4

20 mM to 3.8 mM. For most of stage I, outflow SO_4^{2-} concentrations were below inflow

21 concentrations (Fig. 2). The concentration of NPDOC showed a sharp increase up to

22 38.4 mM during the first 4 days, followed by a rapid decrease to 0.1 mM (Fig. 2). DIC

23 content in the output samples was higher than in the inflow water throughout the

24 experiment, ranging from 6.8 mM to 8.9 mM (Fig. 2).

25 After the 7 week lag period, no NO3- leaching from the compost was observed and NO3-

26 concentrations decreased progressively to values below the detection limit (0.002mM).

27 During this stage, no significant NO_2^- accumulation was observed. The outflow

28 concentration values for NH_4^+ and NPDOC in stage II remained close to the detection

1   limit (0.03 µM and 8 µM), and SO_4^{2-} concentrations were below inflow concentrations by

2   the end of this stage (after 213 days).

3   In the PTC experiment, no significant initial NO_3^- and NO_2^- release was observed (Fig. 3).

4   In contrast to the CCC experiment, a sharp increase in NH_4^+ (up to 6.3 mM after 1 day)

5   was detected (Fig. 4b). Similarly to the CCC experiment, outflow SO_4^{2-} concentrations

6   were below inflow concentrations for most of stage I. NPDOC concentrations remained

7   stable at between 0.1 mM and 0.2 mM and, in contrast to the CCC experiment, there

8   was no sharp increase at the beginning of the experiment (Fig. 3). Output DIC values

9   were lower than input values except on the first day (Fig. 3). After the lag period,

10   complete denitrification was again achieved, although small NO_3^- peaks were observed,

11   probably due to flow rate changes. Similarly to the CCC experiment, no significant NO_2^-

12   or NH_4^+ accumulation was observed and outflow sulphate concentrations were below

13   inflow concentrations by the end of stage II (after 173 days). The main difference was a

14   significant initial NPDOC release (up to 2.5 mM).

15

16   **3.3. Isotopic results**

17   In the CCB experiment, an increase of both $\delta^{15}N$-NO_3^- (from +9.4‰ to +65.6‰) and $\delta^{18}O$-

18   NO_3^- (from +18.6‰ to +52.6‰) was observed as the NO_3^- concentration decreased

19   (Supplementary material, Table S1). In the PTB experiment, the $\delta^{15}N$ of dissolved NO_3^-

20   increased (from +15.40‰ to +32.10‰) as the NO_3^- concentration decreased (Table S1).

21   In the latter experiment, rapid NO_3^- consumption promoted considerable NO_2^-

22   accumulation, hindering the determination of $\delta^{18}O_{NO3}$. A subset of 22 outflow samples

23   from the CCC experiment and 14 samples from the PTC experiment was selected for

24   NO_3^- and NH_4^+ isotopic analyses. In the CCC experiment, the isotopic composition of

25   dissolved NO_3^- showed an increase from +15.0‰ to +61.3‰ for $\delta^{15}N$, and from +10.6‰

26   to +52.2‰ for $\delta^{18}O$ during the first 10 days of stage I, coinciding with the complete

27   consumption of NO_3^- (Supplementary material, Table S3) . In stage II, $\delta^{15}N$ and $\delta^{18}O$

28   increased during the two periods of NO_3^- reduction (up to +60.7‰ and +49.8‰,

1   respectively) (Table S3) separated by a NO_3^- rebound linked to an increase in flow rate

2   up to 0.4 mL min^{-1} (from 154 to 165 days). Stage II of the PTC experiment showed a

3   similar trend to that of the CCC experiment, whereby the isotopic composition of

4   dissolved NO_3^- showed an increase from +16.5‰ to +53.2‰ for $\delta^{15}N$, and from +21.4‰

5   to +62.3‰ for $\delta^{18}O$, coinciding with the complete consumption of NO_3^- (Supplementary

6   material, Table S5). The $\delta^{15}N$ values of dissolved NH_4^+ ranged between +7.1‰ and

7   +11.4‰ in the CCC experiment, whereas a wider range of values was observed in the

8   PTC experiment, from +2.2‰ to +17.9‰ (Fig. 4).

9   The $\delta^{13}C_{DIC}$ was determined in a subset of 28 samples from stage I of the CCC

10   experiment and 15 samples from both stages of the PTC experiment. The $\delta^{13}C_{DIC}$ values

11   ranged from -13.2‰ to -18.6‰ for the CCC experiment and from -10.3‰ to -18.0‰

12   (stage I) and from -16.0‰ to -16.9‰ (stage II) for the PTC experiment. A subset of 25

13   samples from each experiment, with varying SO_4^{2-} concentrations, was analysed to

14   determine the isotopic composition of dissolved SO_4^{2-} ($\delta^{34}S_{SO4}$ and $\delta^{18}O_{SO4}$). In the CCC

15   experiment, the outflow $\delta^{34}S$ and $\delta^{18}O$ values ranged from +7.7‰ to +22.4‰ and from

16   +10.1‰ to +13.6‰, respectively (Supplementary material, Table S3). In the PTC

17   experiment, values ranged from +9.1‰ to +10.6‰ for $\delta^{34}S$, and from +11.2‰ to +11.1‰

18   for $\delta^{18}O$ (Supplementary material, Table S5)

19

20   **4. Discussion**

21   **4.1. Nitrogen - sulphate geochemistry and nitrate attenuation**

22   Complete NO_3^- attenuation was achieved in all the experiments. In the column

23   experiments, the CCC experiment showed an initial NO_3^- release, a temporary NO_2^-

24   accumulation, and a slight NH_4^+ increase, whereas in the PTC experiment very low NO_2^-

25   accumulation and a large initial NH_4^+ increase was observed. This increase in NH_4^+ might

26   indicate NH_4^+ leaching from vegetal decomposition, but could also be generated by

27   DNRA. If NH_4^+ was leached from the organic substrates, its isotopic composition should

1   be in agreement with the reactive material (compost/palm leaves). This was observed in

2   the CCC experiment and in the first days of the PTC experiment (Fig. 4). Therefore, it is

3   reasonable to assume that NH_4^+ leaching was the main source of NH_4^+ observed at the

4   beginning of both experiments. However, by the end of stage I of the PTC experiment,

5    $\delta^{15}N_{NH4}$ values were significantly higher (up to +16.2‰), a finding that could not be

6   explained by leaching. Instead, a feasible hypothesis is the occurrence of DNRA. In

7   general terms, DNRA is favoured under higher C to NO_3^- ratios when the electron

8   acceptor (NO_3^-) becomes limiting and the system is rich in labile carbon (Korom et al.,

9   1992; Burgin and Hamilton, 2007). Accordingly, the highest C/N ratio was observed in

10   the stage I of the PTC experiment when NH_4^+ isotope data discards NH_4^+ leaching and

11   points to the occurrence of DNRA. Nevertheless, DNRA can also occur under low C/N

12   ratios (Carrey et al., 2014). In addition, it seems that the type of organic carbon may have

13   some role in the development of denitrification or DNRA. Further research is needed to

14   better understand which process is taking place. However, the extent of DNRA in the

15   present experiments was limited, since even assuming that NH_4^+ was derived from

16   DNRA, this would only account for a maximum of 15% of NO_3^- attenuation in the PTC

17   experiment. Therefore, the main NO_3^- attenuation process in both experiments was

18   denitrification.

19   The NO_3^- reduction pathway depends on the biomass present in the system, which is

20   controlled by the type of organic carbon available (Nijburg et al., 1998). In addition, Abell

21   et al. (2009) have reported that DNRA bacteria have the capacity to use organic

22   substrates unavailable to denitrifier bacteria. It is reasonable to assume that the

23   differences observed in the two experiments with regard to NH_4^+ generation could be

24   explained by the different organic matter used as electron donor. Palm tree leaves have

25   the capacity to release more NH_4^+ than commercial compost, besides being a labile

26   organic substrate that facilitates NH_4^+ formation through the DNRA process. These

27   results are consistent with the marked differences in NPDOC values obtained in the first

28   sample of the batch experiments: 150 mg L^{-1} for the PTB and 4 mg L^{-1} for the CCB.

1 After the lag period, in stage II of both experiments a faster denitrification was observed.

2 Therefore, it was demonstrated a high denitrification potential for these two types of

3 organic material (CC and PT). These substrates might be used in ARP, where the

4 conditions are variable; even during dry periods, when a potential entry of oxygen might

5 occur.

6 SO_4^{2-} reduction may be promoted when NO_3^-, Mn and Fe have been entirely consumed

7 but organic carbon is still available. The input water contained Fe and Mn concentrations

8 below the detection limit (2 µM and 0.2 µM, respectively); therefore, once the NO_3^- had

9 been completely consumed, SO_4^{2-} reduction could occur according to the redox

10 sequence in natural systems, since most of the organic matter was still available for

11 degradation. For most of stage I and by the end of stage II in both the CCC and PTC

12 experiments, SO_4^{2-} consumption was observed once all the NO_3^- had been removed. In

13 addition, in both experiments, Eh was close to the values that have been reported to

14 promote SO_4^{2-} reduction (below -150 mV, Connell and Patrick, 1968). Isotope results

15 confirmed the occurrence of sulphate reduction (see Supporting material).

16

17 **4.2.   Denitrification rate and organic C reactivity**

18 In order to quantitatively compare the reactivity of the two organic carbon sources, we

19 developed a kinetic model of the two batch experiments. As the observed NO_2^-

20 concentration in the experiments was high (up to 33.4 mg L^{-1}), the model considered two

21 main processes: 1) the degradation of NO_3^- into NO_2^-, and 2) the degradation of NO_2^-

22 into $N_2(g)$. We tested different kinetics during the modelling process, and found that the

23 best combination was zero order kinetics for the degradation of NO_3^- into NO_2^- (Eq. 8)

24 and first order degradation considering inhibition by NO_3^- for the degradation of NO_2^- into

25 $N_2(g)$ (Eq. 9).

26 $r_{NO_3^-} = -K_1$ (Eq.8)

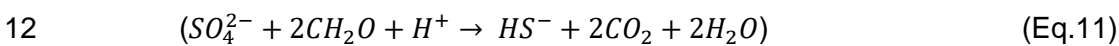27 $r_{NO_2^-} = +QK_1 - K_2[NO_2^-]\left(K_i\big/K_i + [NO_3^-]\right)$ (Eq.9)

14

1   where r is the degradation rate of NO_3^- and NO_2^- [$ML^{-3}T^{-1}$], K_1 is the zero degradation

2   constant [$ML^{-3}T^{-1}$], Q is the stoichiometric ratio between NO_3^- and NO_2^- (1) [-], K_2 is the

3   first order degradation rate [T^{-1}], and K_i is the inhibition parameter [ML^{-3}]. These results

4   contrast with those reported in previous studies, where the model that fit best was the

5   Monod kinetic model (e.g. Rodriguez-Escales et al., 2014; Carrey et al., 2014a). Zero

6   order kinetics is achieved when the substrate is not limiting. In this case, we supposed

7   that organic carbon was not limiting. Note that the amount of organic carbon in the

8   system was much higher than the amount of NO3- (Table 1 and 3). However, the

9   degradation of NO_2^- into $N_2(g)$ was limited by the presence of NO_2^- (first order kinetics

10   with respect to NO_2^-). Both rates were solved numerically considering a time step of 0.5

11   d in the CCB experiment and 0.01 d in the case of PTB. Figure 5 gives the results of the

12   model considering the parameters listed in Table 3 and an initial concentration of NO_3^-

13   of 2.49 mM for CCB and 0.86 mM for PTB. The initial concentrations were based on the

14   initial measurements of the NO_3^- in the batch experiments (see Table S1). Note that the

15   initial NO_3^- concentration in the CCB experiment was higher due to the fast leaching of

16   NO_3^- from the compost. Regarding the parameters, it can be observed that the K_1 value

17   was 10 times higher in the PTB experiment than in the CCB experiment (Table 3),

18   resulting in a characteristic time (i.e. the inverse of the reaction rate constant) of 0.5 days

19   for PTB compared to 3.7 days for CCB. As NO_2^- production in the PTB experiment was

20   much faster than in the CCB one, and NO_2^- degradation rates were relatively similar in

21   both experiments, higher NO_2^- accumulation was expected in the PTB experiment (Fig.

22   5). Kinetic analysis of the column experiments was based on a N input-output mass

23   balance. The NO_3^- concentration in the inflow water (plus NO_3^- nitrate initially leached

24   from the compost and NH_4^+ initially leached from the palm tree leaves) was considered

25   as the input of the system, while outflow concentrations of NO_3^-, NO_2^- and NH_4^+ were

26   considered as the output. Any gaseous species such as N_2O or N_2 were not considered

27   because they were not measured. The percentage of N consumption was calculated for

28   each stage of both column experiments as the difference between the input and the

1   output N masses in the system (Supplementary material, Table S6). During stage I,

2   higher N consumption was achieved with the palm tree leaves than with the compost,

3   although similar N consumption percentages were obtained in both cases after the lag

4   period.

5   Total NO_3^- removed during the experiments was 83.7 mmol for the CCC experiment and

6   139.7 mmol for the PTC experiment, respectively (Table S6). The stoichiometric amount

7   of C needed for the observed NO_3^- and SO_4^{2-} depletion were calculated according to the

8   denitrification reaction (Eq.2), the DNRA reaction (Eq.10) and the sulphate reduction

9   reaction (Eq.11), respectively.

10       $$(NO_3^- + 2CH_2O + 2H^+ \rightarrow NH_4^+ + 2CO_2 + H_2O)$$ (Eq. 10)

11
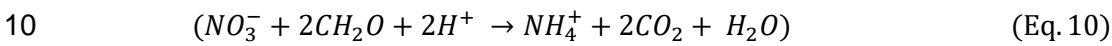
12       $$(SO_4^{2-} + 2CH_2O + H^+ \rightarrow HS^- + 2CO_2 + 2H_2O)$$ (Eq.11)

13   Obtained values (125.3 mmols C for CCC and 194.8 mmols C for PTC) corresponded to

14   0.8% and 3.7% of the total C in both substrates. Degradable organic C, including the

15   organic carbon leached from the substrates, corresponded to 2.4% and 4.2% of the total

16   C present in the commercial compost and palm tree leaves, respectively. Similar reactive

17   organic C percentages have been obtained in other column experiments using fresh or

18   old organic matter (between 2% and 6%, Abell et al., 2009; Carrey et al., 2013).

19   Palm tree leaves gave a higher denitrification yield (i.e. amount of NO_3^-nitrate consumed

20   per amount of available C) than CC (6 versus 33 mmol NO_3^- / mol C_{org}), probably because

21   the organic carbon was easily degradable by the bacteria present in the water, enabling

22   them to grow rapidly and produce complete NO_3^- attenuation in a short period of time.

23   **4.3.   Nitrate isotope fractionation**

24   In the CCB and CCC experiments, denitrification was the only process consuming NO_3^-

25   . In order to calculate the ε_N and ε_O values, all the samples from both batch and column

26   experiments were plotted together due to the similar trends observed. Figure 6 shows

27   the Rayleigh model for CCC and CCB. Using Eq. 9, isotopic fractionations were

1 calculated as -10.8‰ for ε_N and -9.0‰ for ε_O, with a $\varepsilon_N/\varepsilon_O$ of 1.2. Due to the fast rate of

2 NO_3^- consumption and the transient NO_2^- accumulation in the experiments with palm tree

3 leaves, it was not possible to calculate isotopic fractionation in the batch experiments:

4 calculations were therefore based only on the PTC experiment. Furthermore, as DNRA

5 was detected, the isotopic fractionation obtained was an estimation of the isotope ratio

6 changes for both competing processes. The values obtained were ε_N= -9.9‰ and ε_O= -

7 8.6‰ with a $\varepsilon_N/\varepsilon_O$ of 1.15 (Figure 6).

8 The ε_N and ε_O values obtained were almost equal when using compost or palm tree

9 leaves as substrates, despite the different NO_3^- reduction rate and the limited contribution

10 of DNRA in the PTC. With high denitrification rates, some authors have observed lower

11 isotopic fractionation (Mariotti et al., 1988) whereas others have reported higher

12 fractionation (Korom et al., 2012). In the present study, isotopic fractionation did not show

13 any effect related to changes in the attenuation rate, in agreement with previous

14 laboratory experiments (Carrey et al., 2014b). An overview of isotopic fractionation

15 estimated from several laboratory studies is presented in Table 4.

16 The ε_N and ε_O values obtained in the present study fell within the range of values reported

17 in the literature. The ε_N values obtained were at the lower end of induced denitrification

18 experiment values (Knöller et al., 2011; Carrey et al., 2014b). In general, autotrophic

19 denitrification or pure culture experiments have obtained higher ε_N values (in absolute

20 terms) (Table 4). With regard to ε_O, some authors have reported an inverse fractionation

21 ($\varepsilon_O > 0$‰) due to ^{16}O loss during reduction of NO_3^- to N_2O (Casciotti et al., 2002; Toyoda

22 et al., 2005). The ε_O calculated in the present study showed normal fractionation within

23 the range of reported values for heterotrophic denitrification.

24 Recent studies have focused on the $\varepsilon_N/\varepsilon_O$ ratio in order to elucidate different processes

25 affecting isotopic fractionation during NO_3^- reduction (Granger et al., 2008; Knöller et al.,

26 2011). Factors such as pH, salinity or carbon sources have been reported to show no

27 effect on the $\varepsilon_N/\varepsilon_O$ ratio (Granger et al., 2008; Wunderlich et al., 2012). The incorporation

28 of oxygen isotopes from water into NO_3^- and NO_2^- and re-oxidation of NO_2^- to NO_3^- have

1 been observed to modify ε_O in field studies. These processes tend to reduce ε_O values,

2 increasing the $\varepsilon_N/\varepsilon_O$ ratio up to 1.8 - 2.0. In denitrification laboratory experiments, a wider

3 range has been observed, from 0.96 (Carrey et al., 2013) to 2.9 (Knöller et al., 2011).

4 Higher values can be achieved when important NO_2^- accumulation and NO_2^- re-oxidation

5 is produced (Knöller et al., 2011). The $\varepsilon_N/\varepsilon_O$ ratios obtained in the present experiments

6 were of 1.12 for CCB-CCC and 1.15 for PTC. As palm and compost experiments were

7 performed under anaerobic conditions and NO_2^- accumulation only lasted for a few days,

8 re-oxidation of NO_2^- can be ruled out. In addition, due to rapid NO_3^- reduction and the

9 high isotopic composition of $\delta^{18}O_{NO3}$ (up to +62.3‰), the equilibrium isotope fractionation

10 between water and NO_3^- can be considered negligible compared to kinetic isotope

11 fractionation during NO_3^- reduction.

12 Composition of the microbial community can also affect the $\varepsilon_N/\varepsilon_O$ ratio during

13 denitrification (Dähnke and Thamdrup, 2016). Deviations in $\varepsilon_N/\varepsilon_O$ ratios can be produced

14 by different enzymes involved in NO_3^- reduction (Granger et al., 2008). Activity of the

15 periplasmic NO_3^- reductase (Nap) in denitrifying bacteria resulted in a $\varepsilon_N/\varepsilon_O$ value of ~1.6

16 (Granger et al., 2008). However, membrane-bound respiratory NO_3^- reductase (Nar) is

17 more common in classical heterotrophic denitrification and tends to produce $\varepsilon_N/\varepsilon_O$ values

18 of ~1.0 (Granger et al., 2008). The $\varepsilon_N/\varepsilon_O$ ratios obtained in the present experiments were

19 close to 1.0, suggesting a lower influence of periplasmic NO_3^- reductase, in agreement

20 with NO_3^- reduction driven by heterotrophic denitrification. As some DNRA was observed

21 in the palm experiment, a higher $\varepsilon_N/\varepsilon_O$ would be expected, since the reduction of NO_3^- to

22 NO_2^- by DNRA is considered to be mainly catalysed by Nap complex (Kraft et al., 2011).

23 However, the $\varepsilon_N/\varepsilon_O$ observed in PTC was 1.15, similar to compost (1.12), in agreement

24 with the main role of heterotrophic denitrification in NO_3^- attenuation. Likewise, the $\varepsilon_N/\varepsilon_O$

25 ratio in both experiments was close to values obtained in other laboratory experiments

26 involving induced or natural denitrification in freshwater (Granger et al., 2008; Carrey et

27 al., 2013; Carrey et al., 2014b). The published results suggest that denitrification

28 produces ratios of around 1.0 and any deviation can be related to equilibrium isotope

fractionation, re-oxidation of NO_2^- or a different biological pathway of NO_3^- reduction.

Induced denitrification at field scale may be masked by several processes, such as dispersion, diffusion or dilution (mixing) that could change the NO_3^- concentration in groundwater. The isotopic fractionation of N and O for dissolved NO_3^- obtained in lab-scale experiments may be used in future studies to assess system behaviour in the field and optimise full-scale application.

5. Conclusions

This study shows that CC and PT have a satisfactory capacity to promote complete denitrification, even after a lag stage without flow, simulating a dry period. However, a potential drawback in the use of these substrates is the initial NH_4^+ release and the slight NO_2^- accumulation observed suggesting the necessity of a pre-treatment of the material previously to be installed in the MAR system. Overall, the PT gave higher denitrification rate and yield making it suitable for MAR systems in arid and semi-arid climates, where short-term efficient organic substrate is required.

References

Abell, J., Laverman, A.M., Van Cappellen, P., 2009. Bioavailability of organic matter in a freshwater estuarine sediment: long-term degradation experiments with and without nitrate supply. Biogeochemistry 94, 13-28.

Aravena, R., Robertson, W.D., 1998. Use of multiple isotope tracers to evaluate denitrification in ground water: Study of nitrate from a large-flux septic system plume. Ground Water 36, 975-982.

1   Barford, C.C., Montoya, J.P., Altabet, M.A., Mitchell, R., 1999. Steady-state nitrogen

2   isotope effects of N_2 and N_2O production in Paracoccusdenitrificans. Appl. Environ.

3   Microb. 65, 989-994.

4   Bekele, E., Toze, S., Patterson, B., Higginson, S., 2011 Managed aquifer recharge of

5   treated wastewater: Water quality changes resulting from infiltration through the vadose

6   zone. Water Res., 45, 5764-5772.

7   Bouwer, H., 2002. Artificial recharge of groundwater: hydrogeology and engineering.

8   Hydrogeol. J. 10, 121-142.

9   Burgin, A.J., Hamilton, S.K., 2007. Have we overemphasized the role of denitrification in

10   aquatic ecosystems. A review of nitrate removal pathways. Front. Ecol. Environ. 5, 89-

11   96.

12   Carrey, R., Otero, N., Soler, A., Gomez-Alday, J.J., Ayora, C., 2013. The role of Lower

13   Cretaceous sediments in groundwater nitrate attenuation in central Spain: Column

14   experiments. Appl. Geochem. 32, 142-152.

15   Carrey, R., Otero, N., Vidal-Gavilan, G., Ayora, C., Soler, A., Gómez-Alday, J.J., 2014a.

16   Induced nitrate attenuation by glucose in groundwater: Flow-through experiment. Chem.

17   Geol. 370, 19-28.

18   Carrey, R., Rodríguez-Escales, P., Otero, N., Ayora, C., Soler, A., Gómez-Alday, J.J.,

19   2014b. Nitrate attenuation potential of hypersaline lake sediments in central Spain: Flow-

20   through and batch experiments. J. Contam. Hydrol. 164, 323-337.

21   Casciotti, K.L., Sigman, D.M., Hastings, M.G., Böhlke, J.K., Hilkert, A., 2002.

22   Measurements of the oxygen isotopic composition of nitrate in seawater and freshwater

23   using the denitrifier method. Anal.Chem. 74, 4905-4912.

24   Connell, W.E., Patrick jr. W.H., 1968. Sulfate reduction in soil: effects of redox potential

25   and pH. Science 159, 86-87.

26   Dähnke, K., Thamdrup, B., 2016. Isotope fractionation and isotope decoupling during

27   anammox and denitrification in marine sediments. Limnol. Oceanogr. 61, 610-624.

1 DeBeer, D., Schramm, A., Santegoeds, C.M., Kuhl, M., 1997. A nitrite microsensor for
2 profiling environmental biofilms. Appl. Environ. Microbiol. 63, 973-977.

3 Díaz-Cruz, M., Barceló, D., 2008. Trace organic chemicals contamination in ground
4 water recharge. Chemosphere, 72, 333-342.

5 Directive 98/83/EC. Council Directive 98/83/EC of the European Parliament of the 3
6 November 1998 on the quality of water intended for human consumption. Off. J. Eur.
7 Communities L 330, of 5.12.1998, 32-54.

8 Delwiche, C.C., Steyn, P.L., 1970. Nitrogen isotope fractionation in soils and microbial
9 reactions. Environ. Sci. Technol. 4, 929-935.

10 Dogramaci, S.S., Herczeg, A.L., Schi, S.L., Bone, Y., 2001. Controls on δ^{34}S and δ^{18}O
11 of dissolved sulfate in aquifers of the Murray Basin, Australia and their use as indicators
12 of flow processes. Appl. Geochem. 16, 475-488.

13 Ghiglieri, G., Baba Sy, M.O., Yahyaou, H., Ouessar, M., Ouldamara, A., Soler, A., Arras,
14 C., Barbieri, M., Belkheiri, O., Zaied, M.B., Buttau, C., Carletti, A., Da Pelo, S., Dodo, A.,
15 Funedda, A., Iocola, I., Meftah, E., Mokh, F., Nagaz, K., Melis, M.T., Pittalis, D., Said,
16 M., Sghaier, M., Torrentó, C., Virdis, S., Zahrouna, A., Enne, G., 2014. Design of Artificial
17 Aquifer Recharge Systems in semi-arid regions of Maghreb (North Africa). Flowpath –
18 National Meeting on Hydrogeology. Viterbo. *Abstract Volume*: 144-145. ISBN 978-88-
19 907553-4-7.

20 Gibert, O., Pomierny, S., Rowe, I., Kalin, R.M., 2008. Selection of organic substrates as
21 potential reactive materials for use in a denitrification permeable reactive barrier (PRB).
22 Bioresources Technol. 99, 7587-7596.

23 Granger, J., Sigman, D.M., Lehmann, M.F., Tortell, P.D., 2008. Nitrogen and oxygen
24 isotope fractionation during dissimilatory nitrate reduction by denitrifying bacteria.
25 Limnol. Oceanogr. 53, 2533-2545.

26 Grischek, T., Hiscock, K.M., Metschies, T., Dennis, P.F., Nestler, W., 1998. Factors
27 affecting denitrification during infiltration of river water into a sand and gravel aquifer in
28 Saxony, Germany. Water Res.32, 450-460

1 Hosono, T., Alvarez, K., L., Lin, I.T., Shimada, J., 2015. Nitrogen, carbon, and sulfur
2 isotopic change during heterotrophic (*Pseudomonas aureofaciens*) and autotrophic
3 (*Thiobacillus denitrificans*) denitrification reactions. J. Contam. Hydrol. 183, 72-81.

4 Knöller, K., Vogt, C., Haupt, M., Feisthauer, S., Richnow, H.H., 2011. Experimental
5 investigation of nitrogen and oxygen isotope fractionation in nitrate and nitrite during
6 denitrification. Biogeochemistry 103, 371-384.

7 Knowles, R., 1982. Denitrification. Microbiol. Rev. 46, 43-70.

8 Korom, S.F., 1992. Natural denitrification in the saturated zone – A review. Water
9 Resour. Research 28, 1657-1668.

10 Korom, S.F., Schuh, W.M., Tesfay, T., Spencer, E.J., 2012. Aquifer denitrification and in
11 situ mesocosms: Modeling electron donor contributions and measuring rates. J. Hydrol.
12 432-433, 112-126.

13 Kraft, B., Strous, M., Tegetmeyer, H.E., 2011. Microbial nitrate respiration – Genes,
14 enzymes and environmental distribution. J. Biotechnol. 155, 104-117.

15 Kuster, M.; Díaz-Cruz, S.; Rosell, M.; López de Alda, M.; Damià Barceló, D., 2010. Fate
16 of selected pesticides, estrogens, progestogens and volatile organic compounds during
17 artificial aquifer recharge using surface waters. Chemosphere, 79, 880-886.

18 Leverenz, H.L., Haunschild, K., Hopes, G., Tchobanoglous, G., Darby, J.L., 2010. Anoxic
19 treatment wetlands for denitrification. Ecol. Eng. 36, 1544-1551.

20 Maeng, S.K., Sharma, S.J., Lekkerkerker-Teunissen, K., Amy, G.L., 2011. Occurrence
21 and fate of bulk organic matter and pharmaceutically active compounds in managed
22 aquifer recharge: A review. Water Res., 45, 3015-3033.

23 Magee, P.N., Barnes, J.M., 1956. The production of malignant primary hepatic tumours
24 in the rat by feeding dimethylnitrosamine. Br. J. Cancer. 10, 114.

25 Mariotti, A., Landreau, A., Simon, B., 1988. 15N isotope biogeochemistry and natural
26 denitrification process in groundwater application to the chalk aquifer of northern France.
27 Geochim. Cosmochim. Acta 52, 1869-1878.

McIlvin, M.R., Altabet, M.A., 2005. Chemical conversion of nitrate and nitrite to nitrous oxide for nitrogen and oxygen isotopic analysis in freshwater and seawater. Anal. Chem. 77, 5589-5595.

Miller, J.H., Ela, W.P., Lansey, K.E., Chipello, P.L., Arnold, R.G., 2006. Nitrogen transformations during soil-aquifer treatment of wastewater effluent – Oxygen effects in field studies. J. Environ. Eng.-Asce, 132, 1298-1306.

Nijburg, J.W., Gerards, S., Laanbroek, H.J., 1998. Competition for nitrate and glucose between Pseudomonas fluorescens and Bacillus licheniformis under continuous or fluctuating anoxic conditions. FEMS Microb. Ecol. 26, 345-356.

Pehlivanoglu-Mantas, E., Sedlak, D.L., 2008. Measurement of dissolved organic nitrogen forms in wastewater effluents: Concentrations, size distribution and NDMA formation potential. Water Res., 42, 3890-3898.

Robertson, W.D., Vogan, J.L., Lombardo, P.S., 2008. Nitrate removal rates in a 15-year-old permeable reactive barrier treating septic system nitrate. Ground Water Monit. R. 28, 65-72.

Rodríguez-Escales, P., van Breukelen, B.M., Vidal-Gavilan, G., Soler, A., Folch, A., 2014. Integrated modelling of biogeochemical reactions and associated isotope fractionations at batch scale: A tool to monitor enhanced biodenitrification applications. Chem. Geol. 365, 20-29.

Ryabenko, E., Altabet, M.A., Wallace, D.W.R., 2009. Effect of chloride on the chemical conversion of nitrate to nitrous oxide for $\delta 15N$ analysis. Limnol. Oceanogr. 7, 545-552.

Soler, A., Torrentó, C., Barbieri, M., Canals, A., Otero, N., Domènech, C., Carrey, R., Audí-Miró, C., Puig, R., Navarro-Ciurana, D., Rodríguez-Fernández, D., Grau-Martínez, A., de Olamendi, M., Marimón, R.M., Rodríguez, D., 2016. Hydrochemical and Isotopical characterization of the Oued Biskra watershed (Algeria). WADIS-MAR Final conference International Workshop on sustainable water resources management in arid and semi-arid Regions. Available on line at: www.wadismar.eu/images/poster/2.pdf

Spalding, R.F., Exner, M.E., 1993. Occurrence of nitrate in groundwater - A review. J. Environ. Qual. 22, 392-402.

1 Sutka, R.L., Ostrom, N.E., Breznak, P.H., Gandhi, H., Pitt, A.J., Li, F., 2006.
2 Distinguishing nitrous oxide production from nitrification and denitrification on the basis
3 of isotopomer abundances. Appl. Environ. Microbiol. 72, 638-644.

4 Tiedje, J.M., Sexstone, A.J., Myrold, D.D., Robinson, J.A., 1982. Denitrification:
5 ecological niches, competition and survival. Ant. Van Leeuw. J. Micros, 48, 569-583.

6 Torrentó, C., Cama, J., Urmeneta, J., Otero, N., Soler, A., 2010. Denitrification of
7 groundwater with pyrite and Thiobacillus denitrificans. Chem. Geol. 278, 80-91.

8 Torrentó, C., Urmeneta, J., Otero, N., Soler, A., Viñas, M., Cama, J., 2011. Enhanced
9 denitrification in groundwater and sediments from a nitrate-contaminated aquifer after
10 addition of pyrite. Chem. Geol. 287, 90-101.

11 Toyoda, S., Mutobe, H., Yamagishi, H., Yoshida, N., Tanji, Y., 2005. Fractionation of
12 $N2O$ isotopomers during production by denitrifier. Soil Biol. Biochem. 37, 1535-1545.

13 Tsushima, K., Ueda, S., Ohno H., Ogura, N., Katase, T., Watanabe, K., 2006. Nitrate
14 decrease with isotopic fractionation in riverside sediment column during infiltration
15 experiment. Water Air Soil Pollut. 174, 47-61.

16 Valhondo, C., Carrera, J., Ayora, C., Barbieri, M., Noedler, K., Licha, T., Huerta, M.,
17 2014. Behavior of nine selected emerging trace organic contaminants in an artificial
18 recharge system supplemented with a reactive barrier. Environ. Sci. Pollut. R. 21, 11832-
19 11843.

20 Vidal-Gavilan, G., Folch, A., Otero, N., Solanas, A.M., Soler, A., 2013. Isotope
21 characterization of an in situ biodenitrification pilot-test in a fractured aquifer. Appl.
22 Geochem. 32, 153-163.

23 Vidal-Gavilan, G., Carrey, R., Solanas, A., Soler, A., 2014. Feeding strategies for
24 groundwater enhanced biodenitrification in an alluvial aquifer: Chemical, microbial and
25 isotope assessment of a 1D flow-through experiment. Sci. Total Environ. 494-495, 241-
26 251.

27 Wellman, R.P., Cook, F.D., Krouse, H.R., 1968. Nitrogen-15 – microbiological alteration
28 of abundance. Science 161, 269-270.

1   Westgate, P.J., Park, C., 2010. Evaluation of proteins and organic nitrogen in wastewater

2   treatment effluents. Environ. Sci. Technol., 44, 5352-5357.

3   Wunderlich, A., Meckenstock, R., Einsiedl, F., 2012. Effect of different carbon substrates

4   on nitrate stable isotope fractionation during microbial denitrification. Environ. Sci.

5   Technol. 46, 4861-4868.

6

7

8

9   **Figure captions**

10   **Figure 1.** Variation in NO_3^- and NO_2^- concentrations over time in the batch experiments.

11   (a) CCB and ACB experiments. (b) PTB and SCB experiments. Values and error bars

12   represent the mean and standard deviation, respectively, for the three replicate

13   experiments. Input-NO_3^- concentration is also shown.

14   **Figure 2.** Changes in NO_3^-, NO_2^-, NH_4^+, SO_4^{2-}, DIC and NPDOC outflow concentrations

15   over time under variable operating conditions for the CCC experiment. NO_3^- , SO_4^2 and

16   DIC content of the inflow water are also shown (continuous and dashed lines,

17   respectively). Content of NPDOC in the input water was low (0,1 mgL^{-1}).

18   **Figure 3.** Changes in NO_3^-, NO_2^-, NH_4^+, SO_4^{2-}, DIC and NPDOC outflow concentrations

19   over time under variable operating conditions for the PTC experiment. NO_3^-, SO_4^{2-} and

20   DIC content of the inflow water are also shown (continuous and dashed lines,

21   respectively). Content of NPDOC in the input water was low (0,1 mgL^{-1}).

22   **Figure 4.** Changes in NH_4^+ concentration and isotopic composition over time in the

23   outflow of both column experiments. (a) CCC and (b) PTC experiments. In both

24   experiments, dashed lines represent the range of measured values of the $\delta^{15}N$ for each

25   material

Figure 5. Results of the model for the (a) CCB experiment and the (b) PTB experiment. Open symbols represent experiment results, whereas dashed and continuous lines represent model results

Figure 6. (a) and (c) $\delta^{15}N$ and (b) and (d) $\delta^{18}O$ of NO_3^- against the natural logarithm of the NO_3^- concentration of CCB-CCC (upper panels) and PTC (lower panels). Slopes of the regression lines represent ($\alpha-1$), the isotopic fractionation factor for N and O.

Table captions

Table 1. Summary of key parameters of both organic substrates used in the present experiments: CC and PT

Table 2. Experimental conditions of the batch experiments.

Table 3. Kinetic parameters used for modelling batch experiments.

Table 4. Estimated isotopic enrichment factor (εN and εO) obtained in this study and reported in the literature for in situ natural denitrification in laboratory experiments.
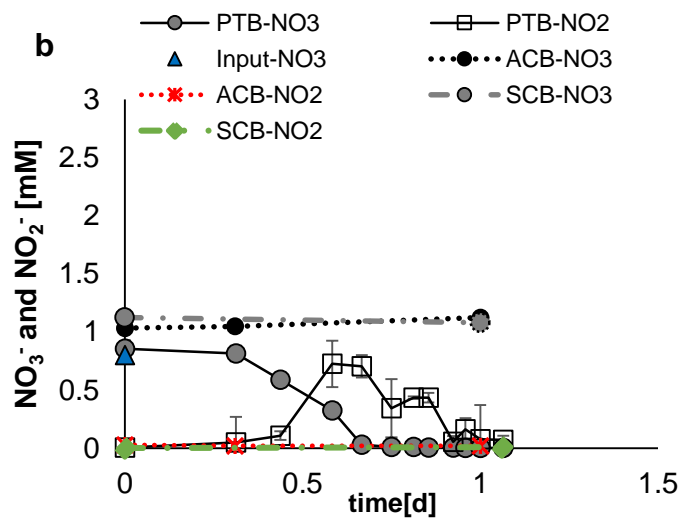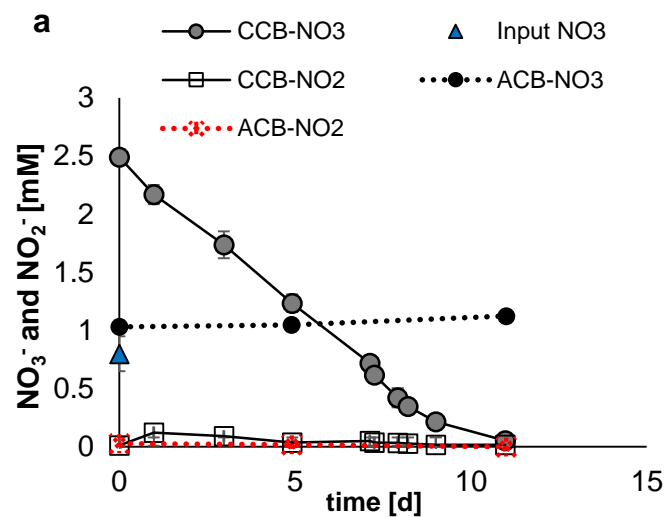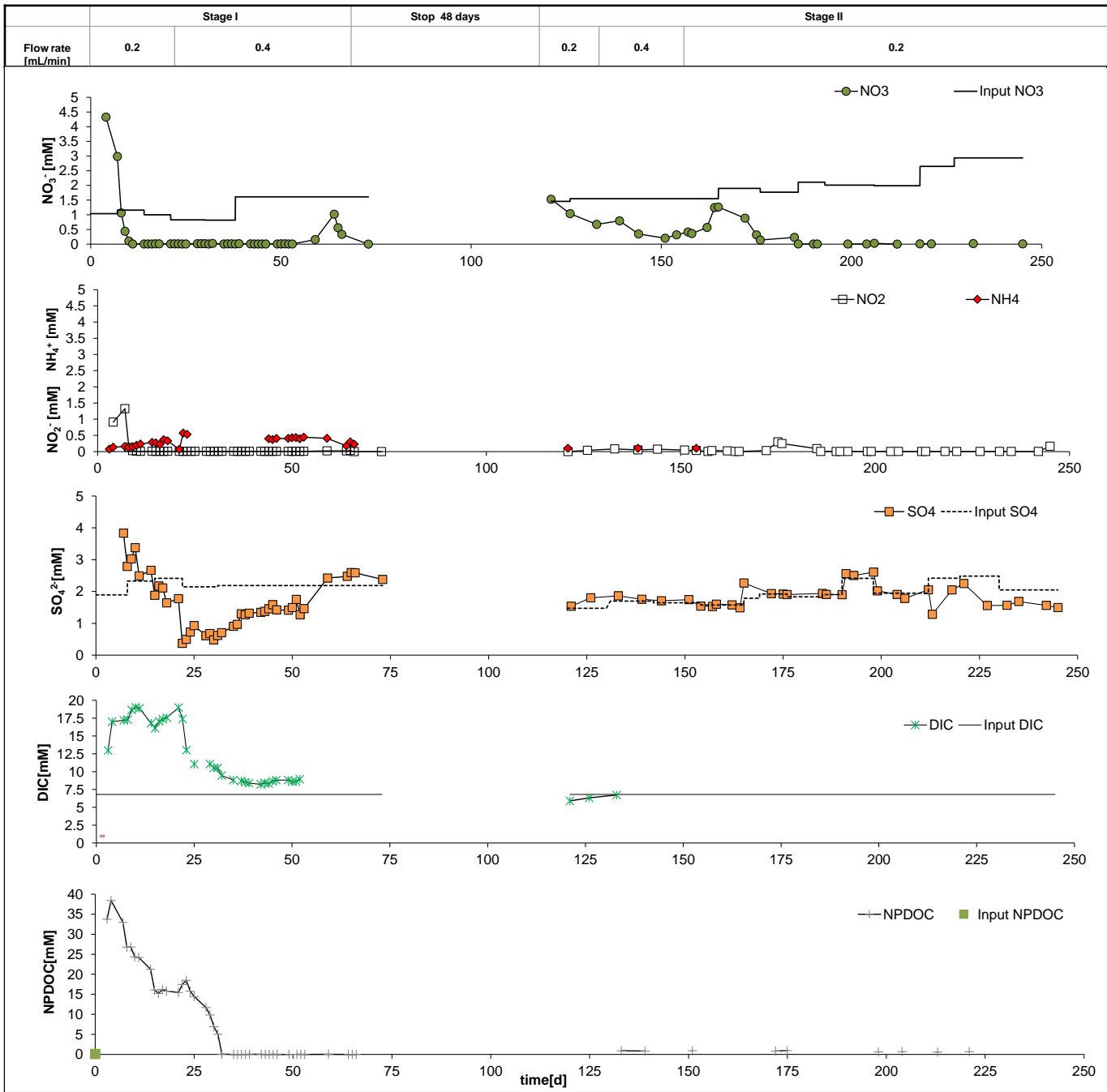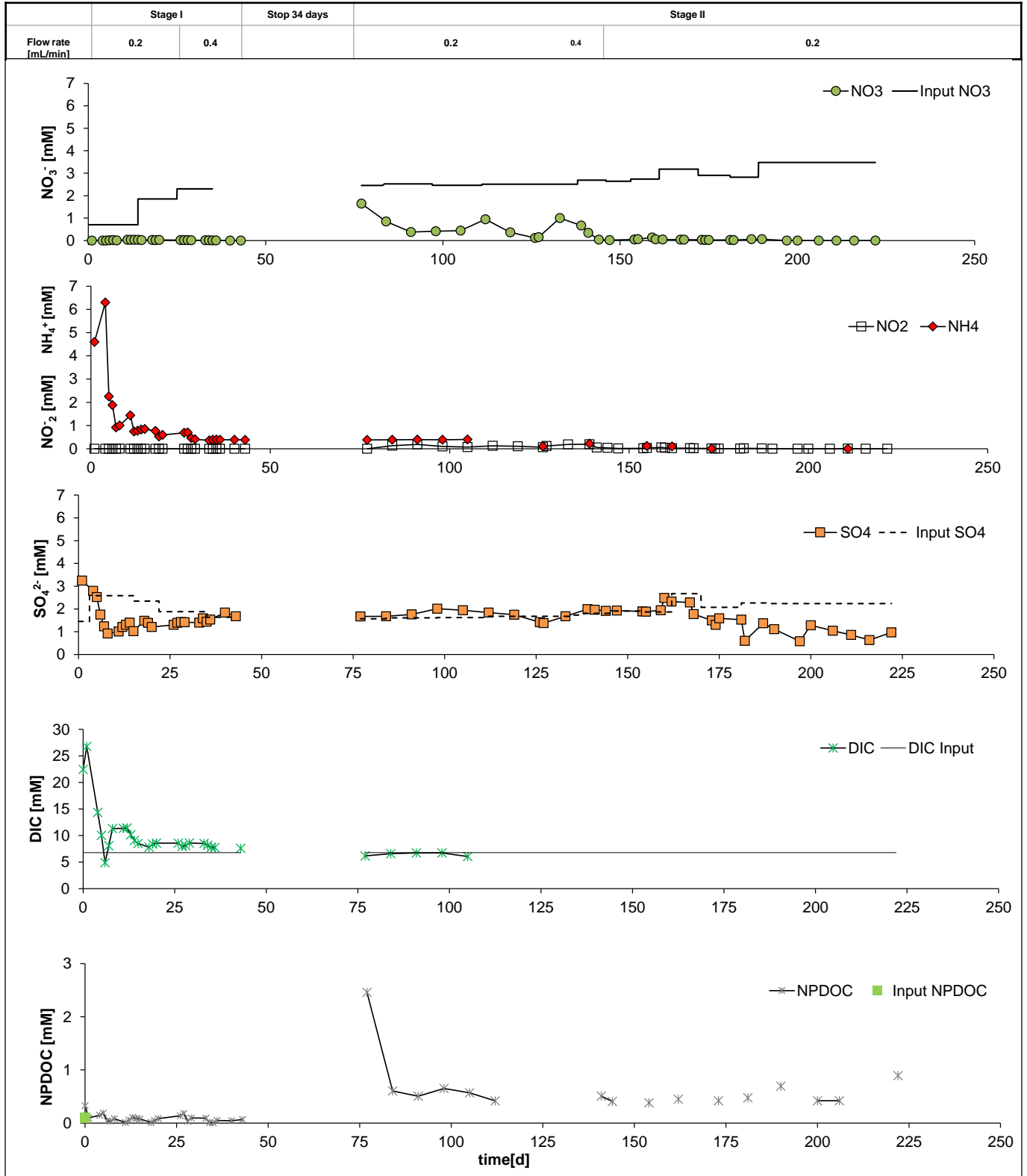
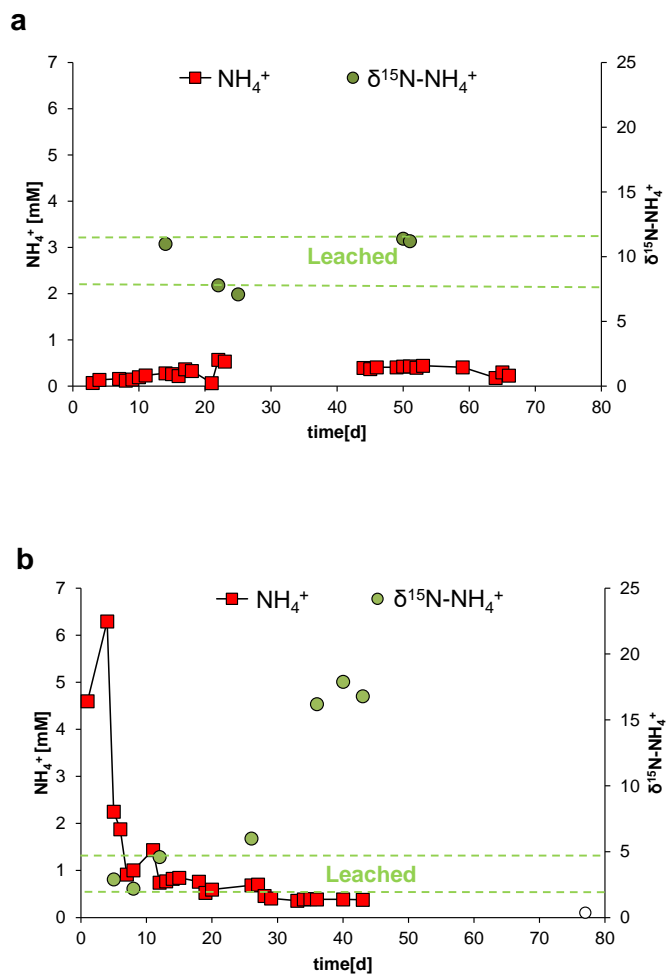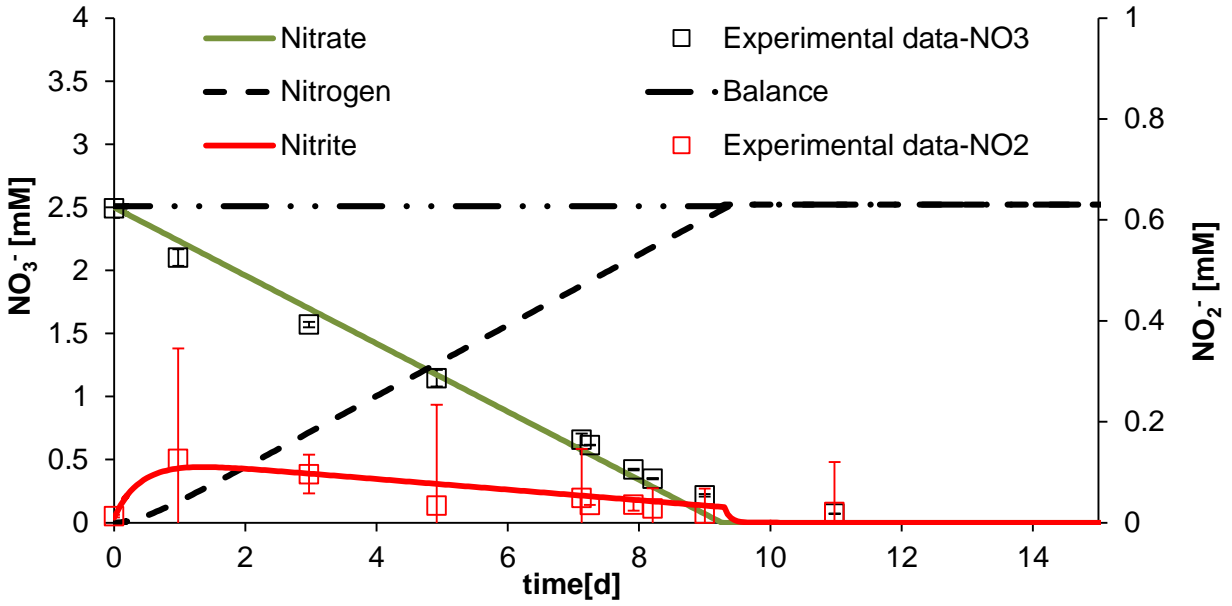# Figure 1

Figure 2

Figure 3
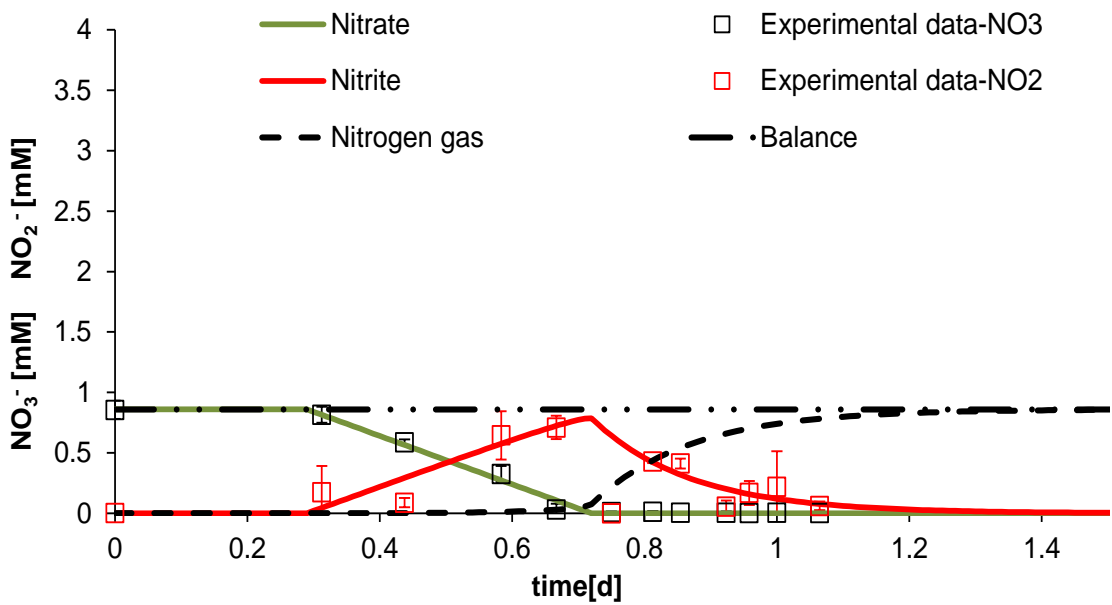
Figure 4

Figure 5

Figure 6

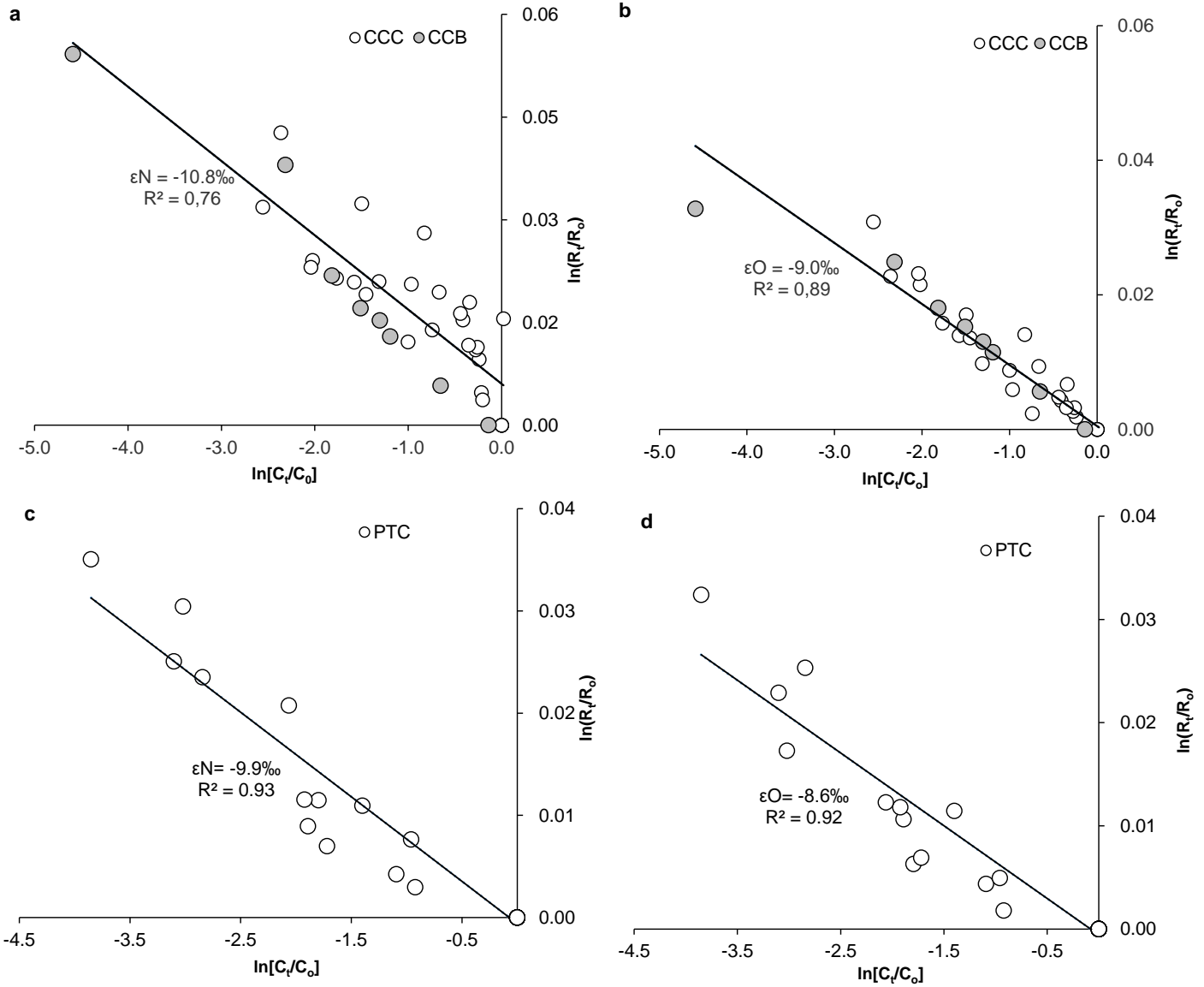**Table 1.** Summary of key parameters of both organic substrates used in the present experiments: commercial compost (CC) and palm tree leaves (PT)

Organic substrate	N(%)	C_{total} (%)	$\delta^{15}N$ (‰)	$\delta^{13}C$ (‰)
CC	1.0±0.2	15.1±1.1	12.1±1.1	-25.1±0.2
PT	1.5±0.6	47.4±0.9	3.6±0.8	-27.1±0.2

Table 2. Experimental conditions of the commercial compost (CCB), sterilized control (SCB), palm tree leaves (PTB) and absence control (ACB) batch experiments

Code	Experiment	Contents of the incubation
CCB	Triplicate (1,2,3)	20 g commercial compost, 400 mL groundwater, 0.80 mM NO_3^-
SCB	Sterilized control	11 g autoclaved crushed palm leaves, 400 mL sterilized groundwater, 0.80 mM NO_3^-
PTB	Triplicate (1,2,3)	11 g palm leaves, 400 mL groundwater, 0.80 mM NO_3^-
ACB	Absence control	400 mL groundwater, 0.80 mM NO_3^-

Table 3. Kinetic parameters used for modelling batch experiments

Experiment	NO_3^- to NO_2^-	NO_2^- to $N_{2(g)}$	
	K_1 (mM d^{-1})	K_2 (d^{-1})	K_i (mM)
CCB	0.27	9	0.8
PTB	2	6.5	0.01

Table 4. Estimated isotopic enrichment factor (εN and εO) obtained in this study and reported in the literature for denitrification lab experiments.

	εN (‰)	εO (‰)	εN/εO	Reference	Commnets
Heterotrophic denitrification					
Pure cultures	-20 to -30	n.d.	n.d.	Wellman et al. (1968)	Batch, Penassay Broth medium, *Psedumonas stutzeri*
	-13.4 to -20.8	n.d.	n.d.	Delwiche and Steyn (1970)	Batch, glucose, *Pseudomonas denitrificans*
	-28.6	n.d.	n.d.	Barford et al. (1999)	Steady-state reactor, acetate, *Paracoccus denitrificans*
	-39 to -31	+13 to +32	n.d.	Toyoda et al. (2005)	Batch, citrate, *Pseudomonas fluorescens*
	-22 to -17	-3 to -1	n.d.	Toyoda et al. (2005)	Batch, citrate, *Pseudomonas fluorescens*
	-22 to -10	+4 to +23	n.d.	Toyoda et al. (2005)	Batch, citrate, *Paracoccus denitrificans*
	-12.7	n.d.	n.d.	Sutka et al. (2006)	Batch, citrate , *Pseudomonas chlororaphis*
	-36.7	n.d.	n.d.	Sutka et al. (2006)	Batch, citrate, *Pseudomonas chlororaphis*
	-18.1 and -17.3	-16.5 and -16.1	1.07 to 1.09*	Wunderlich et al. (2012)	Batch, toluene, *Thauera aromatica* and *Aromatoleum aromaticum*
	-18.9	-15.9	1.19*	Wunderlich et al. (2012)	Batch, benzoate, *Thauera aromatica*
	-22.1 and -23.5	-19.9 and -23.7	1.0 to 1.1*	Wunderlich et al. (2012)	Batch, acetate, *Thauera aromatica* and *Aromatoleum aromaticum*
	-8.6 and -16.2	-4.0 and -7.3	1.26 to 2.94	Knöller et al. (2011)	Batch, succinate and toluene, *Azoarcus sp.* and *Ps. pseudoalcaligenes*
Seawater	-5.4 to -26.6	-4.8 to -22.6	1.0 to 1.8	Granger et al. (2008)	Batch, seawater, pure cultures
Freshwater sediment	-14.6	n.d.	n.d.	Grischek et al. (1998)	Column, sediment from sandy silty and gravel aquifer and river water
	-32.9 to -34.1	n.d.	n.d.	Tsushima et al. (2006)	Column, aquifer sediment and groundwater
	-11.6 and -15.7	-12.1 and -13.8	0.96 to 1.14	Carrey et al. (2013)	Column, organic- and sulfide-rich sediments and groundwater
Freshwater sediment bioestimulated	-17.1	-15.1	1.1	Vidal-Gavilan et al. (2013)	Batch, aquifer material and groundwater + glucose
	-13	-8.9	1.5	Vidal-Gavilan et al. (2013)	Batch, aquifer material and groundwater + ethanol
	-6.5	-6	1.01	Vidal-Gavilan et al. (2014)	Column, aquifer material and groundwater + ethanol
	-8.8	-8	1.1	Carrey et al. (2014)	Column, aquifer sediment and groundwater + glucose
	-10.4	**-9**	**1.3**	**This study**	**Column and batch, groundwater + commercial compost**
	-9.9	**-8.6**	**1.15**	**This study**	**Column, groundwater + palm tree leaves**
Autotrophic denitrification					
	-15.0 and -22.9	-19.0 and -13.5	1.2	Torrentó et al. (2010)	Batch, pyrite, pure culture (*Th. denitrificans*)
	-12.6	-8.8	1.43	Hosono et al. (2015)	Batch, pyrite, pure culture (*Th. denitrificans*)
	-25.0 and -27.6	-13.5 and -21.3	1.3	Torrentó et al. (2011)	Batch, aquifer sediment + pyrite

n.d. = not dertermined, (*) Values estimated from published data